



Semnan University



Review Article

Hydrodynamic Cavitation in the Fuel Injector Nozzle and its Effect on Spray Characteristics: A Review

Mehul P. Bambhanian*, Nikul K. Patel

*Mechanical Engineering Department, Faculty of Technology & Engineering, The Maharaja Sayajirao University of Baroda, Vadodra, India.***PAPER INFO****Paper history:**

Received: 2022-12-02

Revised: 2023-06-20

Accepted: 2023-06-24

Keywords:

Hydrodynamic cavitation;

Fuel injector nozzle;

Spray formation;

Cavitation induced spray;

String cavitation.

ABSTRACT

The performance of internal combustion engines can be improved by optimizing fuel spray characteristics. However, high injection pressures and small nozzle diameters in modern fuel injectors result in cavitation flows inside the nozzle, making it difficult to accurately characterize vapor bubble formation and growth. In this review, we explore the influence of cavitation flow on spray formation and examine the effects of geometric and operational factors. We discuss the experimental techniques used to generate a cavitation map and the mathematical models used to describe the behavior and magnitude of the bubble. We also investigate the impact of cavitation on spray properties, including the enhancement of liquid jet fragmentation due to the collapse of cavitation bubbles near the nozzle output. We present a multidimensional cavitation-coupled spray model and discuss the effect of cavitation on spray angle. While experimental work is effective, theoretical analysis can also provide insights into the impact of cavitation flow on spray characteristics. Our review concludes that the spray angle increases during the growing cavitation and super cavitation regimes, but decreases significantly following the cavitation flip. The string cavitation is observed when the position of the needle valve shifts or at a lower needle lift and the spray cone angle increases significantly. Overall, this review provides an inclusive overview of cavitation flow and its influence on spray formation and will aid in the development of more efficient internal combustion engines.

DOI: [10.22075/jhmtr.2023.29165.1406](https://doi.org/10.22075/jhmtr.2023.29165.1406)

© 2023 Published by Semnan University Press. All rights reserved.

1. Introduction

The rapid growth in energy demands increases carbon emissions and leads to the risks of the global warming effect. According to the projection, about 40% of energy sources will come from liquid fuels by 2040 [1]. A major portion of liquid fuel is used in the transportation sector with the Internal Combustion (IC) engine. Efficient fuel combustion is the prime requirement of both diesel & gasoline engines. Although, both engine technologies are evolving to satisfy two major requirements: Fuel efficiency, & Emission reduction. The emission of the diesel engine can be reduced by efficient fuel atomization i.e. producing smaller and more dispersed fuel droplets.

Producing smaller and more dispersed droplets leads to complete combustion of the fuel-injected, resulting in less emission production. Thus the flow of fuel inside the fuel injector nozzle is to be known to have a considerable effect on the spray [2].

Modern injectors for passenger cars and heavy-duty engines are working at 2000 bar injection pressure and inject the liquid fuel through the orifice of diameter in the order of 100 to 300 μm [3]. The liquid fuels enter the combustion chamber in the form of a fuel jet with velocities of around 500 m/s. The liquid fuel jets start to break into liquid ligaments, immediately after leaving the nozzle orifice. This phenomenon is called primary break-up. In addition,

*Corresponding Author: Mehul P. Bambhanian.

Email: mehul.bambhanian-med@msubaroda.ac.in

liquid ligaments break into droplets and further break up forming a dense spray. During high injection pressure, fuels flowing inside the fuel injector nozzle holes observed turbulence and cavitation phenomenon leading to a primary break-up. Cavitation is one of the important phenomena happening inside the fuel injector nozzle leading to primary break-up. The primary breakup is an important phenomenon for the atomization and combustion of fuel inside the combustion chamber of an IC engine. In this paper, an effort is made to compile the work carried out by various researchers using experimental and numerical approaches were summarized. The extent of work carried out by various researchers shows the potential of the cavitation phenomenon leading to primary break-up. The following sections enumerate results and discussions of the cavitation phenomenon assessed experimentally and numerically by different researchers.

The present work is organized in this way. The physics behind the cavitation flow and its governing parameters has been explained in the first section. The second section summarizes the various experimental work and their limitations in using the scaled-up and real-size nozzle. The third section explains various cavitation models which are categorized as the one-dimensional model, single-fluid model, barotropic model, mass transport model and multi-fluid model with their bubble dynamics. The effect of cavitation flow on the spray formation has been discussed in the fourth section. The recently developed cavitation coupled spray models and their limitations have been reviewed. In addition, vortex induced cavitation has been discussed. Finally based on this review important conclusions are summarized in the last section of the paper.

1.1. Cavitation in the Fuel injector nozzle

Hydrodynamic cavitation can be defined as a phenomenon in which the formation of bubbles takes place in a liquid when the static pressure drops below the vapor pressure. Consider incompressible, frictionless, isothermal one-dimensional flow as shown in Fig. 1. Schmidt et al. [5] used the Bernoulli equation to explain the fact.

$$p_1 + \frac{\rho u_1^2}{2} = p_2 + \frac{\rho u_2^2}{2} \quad (1)$$

When the fluid flow through the nozzle from point 1 to point 2, the flow velocity (u) increases, as well as static pressure (p) decreases along the length. At the inlet edge (vena-contracta) the minimum static pressure has been reached, which creates a recirculation zone. The recirculation zone is filled with vapor bubbles when the local pressure reaches below vapor pressure. An additional effect enhancing the inception of cavitation in this low-pressure zone is the

high shear flow generated by the large velocity gradients in the region between the recirculation zone and the main flow. This shear flow generates a high level of turbulence. The cavitation area that forms at the nozzle wall eventually splits away from the wall and decomposes into bubble clusters. As soon as the local pressure exceeds the vapour pressure, the bubbles will begin to collapse downstream.

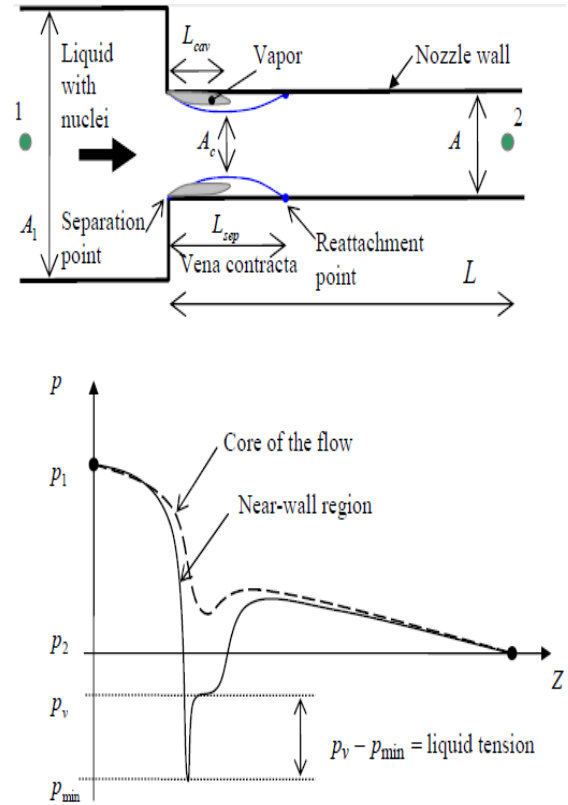


Figure 1. Sketch of nozzle entrance that shows the cavitation inception, Jean et al. [6]

The rise in the injection pressure increases the intensity of the cavitation. Based on the injection pressure the inner nozzle flow can be classified into different flow regimes: no cavitation or turbulent flow, cavitation inception flow, cavitation growth flow, super-cavitation flow, and hydraulic flip flow.

Fig. 2 is a schematic of the evolution of cavitation flow [7]. The cavitation bubbles start to generate at the nozzle entrance when the local pressure reaches the critical value, as shown in Fig. 2(a). the cavitation region developed with pressure and extends to the outlet of the nozzle is known as the supercavitation, as shown in Fig. 2(c). The cavitation bubbles collapse as it comes out from the nozzle and increases the turbulence within the liquid jet. The further rise in injection pressure leads to gas entrainment into the nozzle creating a thin layer of gas attached to the wall and cavitation disappears immediately. This is known as hydraulic flip, as shown in Fig. 2(d).

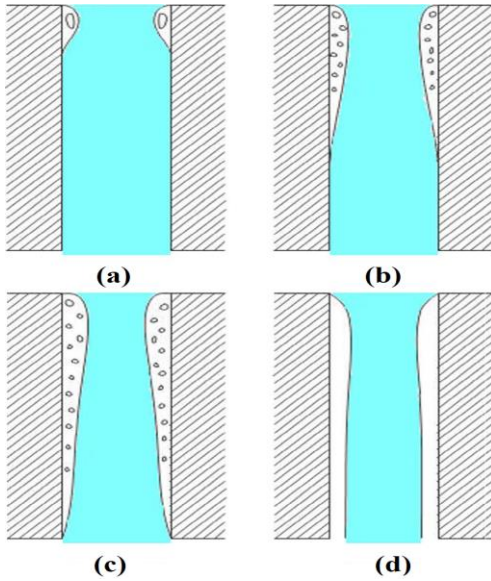


Figure 2. Evolution of cavitation flow inside fuel injector nozzle, (a) cavitation inception, (b) cavitation growth, (c) supercavitation, (d) hydraulic flip, Cui et al. [7]

The two important non-dimensional numbers that are used to characterize cavitation nozzle flows are Cavitation Number (CN) and Discharge coefficient (C_d). The cavitation number is one of the criteria frequently used to determine the appearance of the cavitation and is given by:

$$CN = \frac{p_{inj} - p_{back}}{p_{inj} - p_v} \quad (2)$$

where p_{inj} , p_{back} , and p_v are the injection pressure, back pressure and vapour pressure, respectively. A large value of the CN suggests non-cavitation flow while a small CN corresponds to strong cavitation flow. The critical cavitation parameter is defined as CN_{crit} , which represents cavitation starting to occur at corresponding pressure drops. Cavitation flows, characterized by highly fluctuating spatial topology on a small time scale, are unsteady. In the fuel injection process the nozzle geometry, needle lift, injection pressure, and back pressure considerably influence the mass flow rate of the fuel and the cavitation phenomenon. The efficiency of the fuel injector nozzle can be represented in terms of a non-dimensional parameter called the discharge coefficient (C_d). The discharge coefficient (C_d) is the ratio between the actual mass flow rate and the ideal mass flow rate based on loss-free conditions and can be calculated based on Bernoulli's equation as below:

$$C_d = \frac{\dot{m}_{actual}}{\dot{m}_{ideal}} = \sqrt{\left(\frac{\frac{1}{2} \rho u^2}{P_{inj} - P_{back}} \right)} \quad (3)$$

where \dot{m}_{actual} is the actual mass flow rate through the nozzle, and \dot{m}_{ideal} is the ideal mass flow rate calculated by combining the Continuity and Bernoulli's equation and given by:

$$\dot{m}_{ideal} = A_0 \sqrt{2\rho(P_{inj} - P_{back})} \quad (3a)$$

(for non-cavitating flow)

$$\dot{m}_{actual} = C_c A_0 \sqrt{2\rho(P_{inj} - P_v)} \quad (3b)$$

(for cavitating flow)

where A_0 and ρ are the outlet area of the nozzle and fluid density, respectively. C_c is the coefficient of contraction. Using the above equation, the coefficient of discharge can be written as:

$$C_d = \frac{\dot{m}_{actual}}{\dot{m}_{ideal}} = C_c \sqrt{\left(\frac{P_{inj} - P_v}{P_{inj} - P_{back}} \right)} = C_c \sqrt{K} \quad (4)$$

where K is defined as the Cavitation parameter, which is different from CN and used by Nurik [9]. When the injection pressure of fuel is very high as compared to backpressure K tends to become unity, which leads to $C_d \approx C_c$. Therefore, the discharge coefficient at high injection pressure will become equal to the coefficient of contraction. C_c can be defined as the ratio of the effective area of the liquid jet emanating from the nozzle to the actual exit area of the nozzle. The shape (cylindrical, conical) and size (length, diameter) of the fuel injector nozzle has a considerable effect on C_d . Moreover, the sharp edge inlet, rough edge inlet and rounded inlet show more influence on the discharge coefficient. The cavitation can be used to identify the inner nozzle flow's characteristics. It is widely accepted that there is a close relationship between spray formation and primary breakup. The combination of three mechanisms controls the primary breakup of the liquid jet (a) Aerodynamic forces experienced by the liquid jet (b) Turbulence within the liquid phase (c) Cavitation bubbles shown in Fig. 3 [3]. The spray characteristics can be understood by the macroscopic parameter like the Spray cone angle and Spray tip penetration as well as the microscopic parameter like droplet size distribution and velocity distribution.

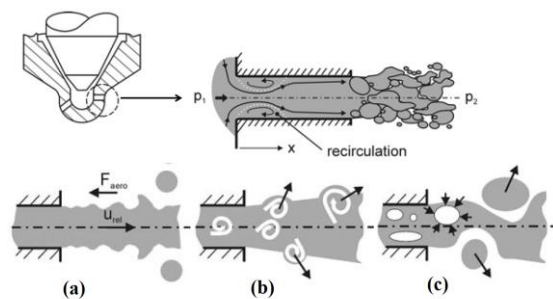


Figure 3. Governing mechanism for primary spray break-up, Baumgarten [3]

The objective of the current study is to provide an extensive review of the various parameters affecting

the cavitation flow inside the fuel injector nozzle and its consequent effect on the spray characteristics. The entire review is divided into three sections. In the first section, Experimental work has been reviewed for inner nozzle cavitation. In the second part, the analytical and computational fluid dynamic (CFD) model has been reviewed along with the commercial CFD software. The last section covered the coupling methodology between cavitation and spray formation as well as the effect of cavitation on spray formation.

2. Experimental Study on Cavitation Flow

Several experimental literature works have been published to determine the behaviour of the cavitation flow in the fuel injector nozzle. This experiment helps to understand the structure of cavitation and the two-phase flow pattern. The results of the experimental investigation confirm a significant impact on nozzle efficiency due to cavitation. There is significant progress in the clarification of the structure of cavitation flow inside the nozzle due to studies carried out by several researchers like Bergewerk [8], Nurik [9], Soteriou et al. [10], Chaves et al. [11], Schmidt et al. [12], Arcoumaniset et al. [13], Winklhofer et al. [14], Payri et al. [15], Sou et al. [16], and Mauger et al. [17]. These studies throw light on the cavitation phenomena inside nozzles, in particular on the identification of a pattern of quasi-steady-state cavitation flow.

An early pioneer experimental work has been carried out by Begewerk [8] in which he discussed the correlation between fuel injection and cavitation. With the help of the flow visualization technique, the flow through a large size transparent nozzle was observed. The presence of cavitation and hydraulic flip mainly depends upon the CN and has little dependence on the Reynolds number. When the liquid flow entirely separates from the nozzle wall and downstream gas enters the nozzle is known as the hydraulic flip condition. Nurik [9] experimented with a scaled-up transparent nozzle ($d \approx 8\text{mm}$) and observed that cavitation and hydraulic flip depend on CN , nozzle radius, length-to-diameter ratio and pressure difference as shown in Fig. 4. By adjusting the nozzles' L/d ratios and pressure differential, experiments have been carried out. Based on his research, he has created an empirical association between the nozzle's cavitation characteristics and discharge coefficient. Soteriou et al. [10] experimented with the large-scale transparent injector nozzle to explore the different flow regimes and the mechanism of its formation inside the nozzle. He emphasizes the effect of hydraulic flips on spray atomization. The flipped nozzle does not experience any wall shear, which leads to poor spray atomization. This condition reduces the turbulence and smooth unbroken liquid jets that come out from the nozzle outlet.

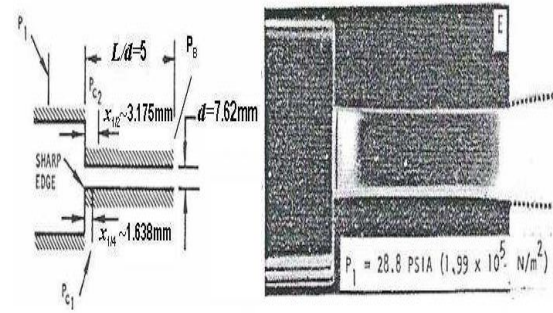


Figure 4. Cavitation in the transparent nozzle observed by Nurik [9]

Although hydraulic flip had never been observed in real scale nozzles with realistic operating conditions. Chaves et al. [11] extended the work conducted by Soteriou et al. [10] with a small-scale nozzle ($d=0.2\text{mm}$) and injection pressure up to 1000 bar. In his work, he reported super cavitation is different from the hydraulic flip. Supercavitation is referred to when cavitation bubbles reach the nozzle's outlet. In this condition, bubbles collapse at the nozzle exit which is a favourable condition for primary spray breakup. Because there won't be any shear resistance at the nozzle wall, there will be a higher liquid velocity there, which allows the jet to escape the nozzle more quickly. Chaves et al. [11] compared their observations with Soteriou et al. [10] with a large-scale nozzle. Based on these observation Chaves et al. [11] speculated that the bubble has its length scale, and do not scale up in large models. This is due to the lifetime of the cavitation bubble which in the real-size nozzle is similar to the large-size nozzle. Thus the interaction between the nozzle flow and cavitation phenomena is completely different in large and real-scale nozzles. Cavities were detected on a small size, however, bubbles could be seen on a big scale, indicating that bubbles have their length scales independent of the nozzle's length scale. Although Soteriou et al. [10] showed that the coefficient of discharge does not depend on the scale of the model. Due to lack of clarity, there is confusion persists to understand the cavitation behavior and flow pattern at different length scales.

Arcoumaniset et al. [13] experimented with large-scale and real-scale acrylic multi-hole injectors. He found that in real-scale experiments there were clear voids were observed and in scaled-up experiments, cloudy bubbles appeared as shown in Fig. 5. He also found that the cavities are initially clear and become more opaque towards the exit of the real scale nozzle. The results indicate that the nature of cavitation changes from a large void to a bubbly mixture in scaled-up experiments. However, Schmidt et al. [5] pointed out that the scattering of light from the cavity surfaces may make large void appears as small bubbles. It is complicated to interpret the image which is subjected to multiple scattering of illuminating light. There is no well-established list of non-dimensional

parameters that govern the cavitation flow, limiting the scaling of the experiment. Experimental results have shown that the real flow does not always follow the classical scaling theory. The scale effect is caused by liquid quantity, bubble dynamics, geometrical differences due to wall roughness, specific flow regimes, cavitation nuclei etc.

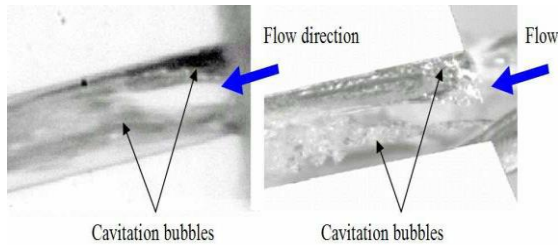


Figure 5. Comparison of hole cavitation for the enlarged (left with $CN=5.5$) and the real size (right with $CN=5.4$) nozzle, Arcoumanis et al. [13]

To develop a complete understanding of cavitation flow and its behaviour, qualitative information in a real-size nozzle is essential. However direct observation of cavitation flow in the real condition is difficult due to very small space and time parameters. To observe cavitation in a real-size nozzle, it must be transparent and capable to withstand high injection pressure and choking condition. A good-quality cavitation image will be convenient for the reader as well as for model validation. But as a matter of consequence, only a few experimental works have been found with the above measures. The nozzle flow is visualized by using a shadowgraph technique, schlieren methods, interferometry imaging, Laser doppler velocimetry (LDV), X-ray, computed tomography (CT), X-ray radiography, laser light sheet illumination etc.

Winklhofer et al. [14] experimented with a real-size two-dimensional throttle (transparent rectangular cross-section) working with European diesel fuel as shown in Fig. 6(a). A set of optical methods was developed and applied for diagnostics of high-pressure diesel flow at transient conditions by using interferometry imaging shown in Fig. 6(b). They are using three different nozzles named J, U and W throttle with different outlet contractions i.e. 0 %, 5 %, and 10 %, respectively. They took more than 20-30 backscattered images of two-phase flow at various pressure differences, and also measured velocity profile with the use of the fluorescence tracking method. Additionally, they employed a distinct colour scheme to distinguish between cavitating, non-cavitating, and foamy (both liquid and gaseous) zones, using blue, red, and yellow hues, respectively. They measured values of the mass flow rate of diesel at the different operating conditions and predicted cavitation inception and choking conditions. They observed that values of mass flow rate in all three types of nozzles (throttle J, U & W) at cavitation inception and choked

flow are almost equal even under different operating conditions. The throttle outlet contraction has an influence on pressure distribution within the nozzle and the growth of cavitation regimes. Mauger et al. [17] also experimented with a similar type of transparent two-dimensional micro-channel using a test oil as shown in Fig. 6(c). A Schlieren technique has been used to measure density gradient at low pressure, however, the technique does not allow density field reconstruction during high-density gradient. A combination of Schlieren and interferometry imaging techniques have been proposed to reconstruct the density field shown in Fig. 6(d). The outcome demonstrates that the cavitation inception is located relatively far from the inlet corner in the shear layers between the recirculation zones and the main flow.

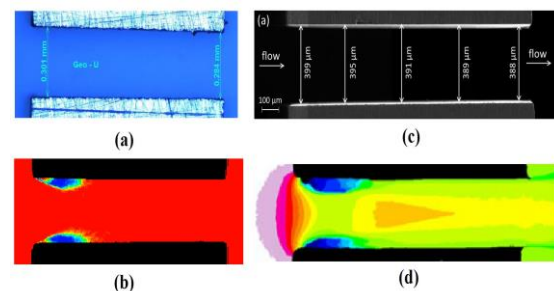


Figure 6. Two-dimensional throttle geometry & cavitation field using interferometry imaging, Winklhofer et al. [14](a,c) & Mauger et al. [17] (b,d)

The physical mechanism behind the initiation, growth, and subsequent bubble collapse of cavitation is investigated using a reduced experimental setup. Results from simplified 2D geometry and simplified working conditions, however, cannot be applied directly to the actual diesel fuel injector nozzle. Few researchers used the real shape and size of the fuel nozzle to study the phenomena of cavitation experimentally. Payri et al. [15] used a single-hole transparent cylindrical nozzle made of fused silica (SiO_2) with an outer diameter of 0.51mm and 1mm in length as shown in Fig. 7. Four different fuels, n-dodecane, n-heptane, n-decane, and commercial diesel, have been used for visualization and parametric study of cavitation flow. The inception of cavitation appears early with low viscous fuel. It is also important to study the effect of geometry shape on the cavitation flow. Cui et al. [18] used a transparent single-hole nozzle to investigate the diameter error, conicality and incline effect, which is commonly found in nozzle geometry. The geometry dimensions were ultra-precisely measured with a micro-hole measuring system. Eleven different shapes of the nozzle geometry ($d=0.8$ mm to 1.2 mm) were used to visualize the internal flow and their hydraulic characteristics were analyzed. They observed that very small differences in geometric structure lead to different characteristics of cavitation flow.

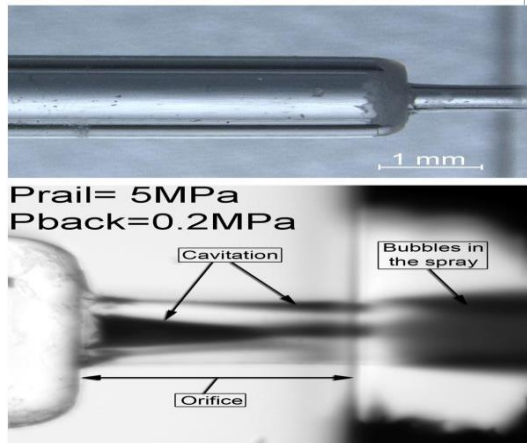


Figure 7. Real size single hole transparent cylindrical nozzle ($d=0.51$ mm, $L=1$ mm) used by Payri et al. [15]

A transparent nozzle involves the limitation of high injection pressure due to higher material stress generated within the nozzle wall. Transparent materials can be either ductile (e.g. Acrylic glass) or brittle (e.g. Sapphire or fused silica). Although acrylic is easily machined, it cannot be used in applications requiring high pressure or temperature. The sapphire or silica is difficult to machine with the conventional machining method. Kirsch et al. [19] proposed the Selective Laser Etching (SLE) method for machining the fused silica. A single-hole transparent nozzle ($d=0.3$ mm, $L=1$ mm) has been used to investigate internal nozzle flow and its effect on spray characteristics with a maximum injection pressure of 250 bar as shown in Fig. 8.

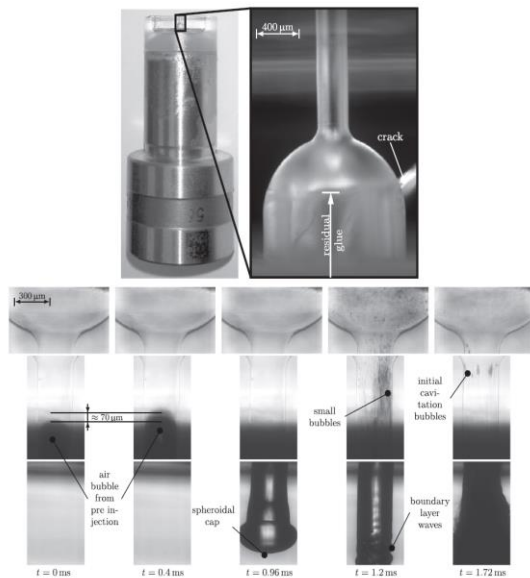


Figure 8. Transparent nozzle ($d=0.3$ mm, $L=1$ mm) fabricated by Selective Laser Etching (SLE) method to withstand 250 bar of pressure used by Kirsch et al. [19]

They photographed the transverse waves on the jet surfaces, the mushroom-shaped spray tip, the early reverse flow, and air bubbles inside the nozzle. Experimental work carried out with a real-size nozzle for cavitation flow is summarized in Table 1.

3. Computational Study on Cavitation Flow

3.1. One-Dimensional Modelling of Cavitation Flow

Nurik [9] experimented by varying pressure difference and L/d ratio with his transparent nozzle. Based on this work he has proposed a one-dimensional theoretical model for predicting the discharge coefficient given below:

$$C_d = C_c \sqrt{K} \quad (4)$$

where $K = \frac{P_{inj} - P_v}{P_{inj} - P_{back}}$ is Cavitation parameter and C_c is the contraction coefficient.

The discharge coefficient (C_d) linearly increases with the cavitation parameter (K) during the cavitation flow. Nurik [9] considered the cavitation flow through a sharp edge nozzle and denoted inlet, outlet and core of the nozzle by points 1, 2 and c, respectively as shown in Fig. 1.

When liquid passes through the minimum cross-sectional area of the nozzle cavitation phenomenon is observed. The values of C_c depend on geometrical parameters, for the sharp edge nozzle it is 0.61 and for the rounded corner, it is between 0.61 to 1. The value of C_c can be calculated with the help of the equation proposed by Weisbach [20].

$$C_c = 0.63 + 0.37 \left(\frac{A_2}{A_1} \right)^3 \quad (5)$$

Although during non-cavitation flow C_d is not a function of K . Lichtarowicz et al. [21] predicted the coefficient of discharge for non-cavitating nozzles by assuming the flow is fully expanded to fill the nozzle. Based on this assumption, the discharge coefficient is a constant value of about 0.84.

When the discharge coefficient (C_d) and cavitation parameter (K) plot on the log-log scale, initially C_d increases with K and then remains constant as shown in Fig. 10. Nurik [9] confirmed this trend through his experiments. Schmidt and Corradini [5] have collected data from similar experimental work and shown them as the graph shown in Fig. 9. The findings support the 1D model put forth by Nurik [9], and it's also noteworthy that the data lie above the predicted curve.

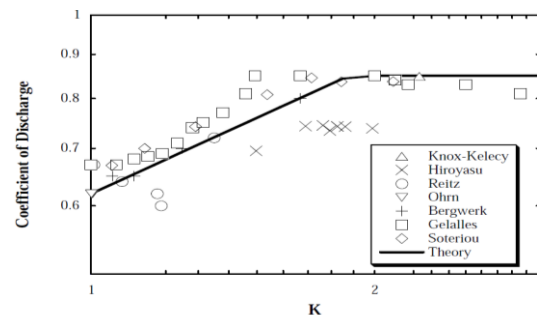


Figure 9. Compilation of experimental nozzle discharge coefficient. Data are plotted on log-log axes, Nurik [9]

Table 1. Summary of experimental work for cavitation flow with real-size nozzle

Author	Nozzle dimension	Operating pressure	Nozzle material	Visualization technique
Winklhofer et al. [14]	$H=0.3$ mm, $L=1$ mm (2D nozzle)	$P_{inj}=100$ bar $P_{back}=20$ to 80bar	Steel sheets are sandwiched between a pair of sapphire windows	Highspeed CCD camera with 500ns of exposure time with imaging interferometry
Maugeret al. [17]	$H=0.4$ mm, $L=1.475$ mm (2D nozzle)	$P_{inj}=50$ bar $P_{back}=1$ bar	Metal sheets are sandwiched between a pair of glass windows	CCD camera with double pulse laser to capture the image. A shadowgraph technique, the Schlieren method, and interferometry imaging have been used.
Payri et al. [15]	$d=0.51$ mm $L=1$ mm	$P_{inj}= 50$ bar, $P_{back}=1$ to 15 bar	Fused silica	CCD Camera with 1280X1024 pixels, 1 μ s of exposure time
Cuiet al. [18]	$d=0.8$ to 1.2 mm (Five nozzle configurations)	$P_{inj}=2$ to 10 bar	Transparent nozzles of polymethyl methacrylate	High-speed CCD camera with LED light
Kirschet al. [19]	$d=0.3$ mm, $L=1$ mm	$P_{inj}=250$ bar, $P_{back}=1.5$ bar	Fused silica has been fabricated with the Selective Laser Etching (SLE) method.	High-speed CCD camera with 1280X1024 pixels (25000fps) (1 μ s exposure time)
Maninet al. [105]	$d_{in}=0.186$ mm, $d_{out}=0.189$ mm $L=1$ mm (ECN Spray A)	$P_{inj}=1000$ bar, $P_{back}=20$ bar	Acrylic nozzle, tip made by micromachining	Two high-speed cameras (2 μ s exposure time) with microscopy lense

The effect of rounding at the inlet increases the coefficient of discharge. Nurik [9] also observed that as K decreases the value of Cd suddenly decreases due to hydraulic flip phenomena, which is also confirmed by Rietz [22]. However, super-cavitation has been observed instead of hydraulic flip in real scale nozzle with realistic operating conditions. The super-cavitation leads to a choked flow condition in which an almost constant mass flow rate is observed with changes in pressure difference.

3.2. Multi-Dimensional Modelling of Cavitation Flow

The one-dimensional model is preferably good to predict the discharge coefficient with a sharp inlet nozzle but does not give much detail about the internal flow behaviour of the cavitation phenomena. An extensive multi-dimensional numerical model is required to gather information about flow parameters within the nozzle as well as at the outlet of the nozzle, which can later be used to model spray characteristics. Many researchers proposed two-phase numerical models for cavitation flow. These models are capable to calculate the temporal behaviour of cavitating flow with the real-size nozzle geometry, which is fairly expensive with the experiments

3.2.1. Bubble Dynamics

Fundamentally, cavitation is the phenomenon in which the bubbles grow when the local pressure is lower than the vapour pressure and collapse if the local pressure is more than the vapour pressure. One of the oldest models for bubble growth and collapse was developed by Rayleigh [23]. He considered a spherical liquid bubble with an initial radius of R_0 , with an empty surrounding. The pressure at the cavity wall was zero and the pressure at a distance of infinity was a constant, P_∞ . The bubble would collapse in time, t is given by:

$$t = 0.915 R_0 \sqrt{\frac{\rho}{P_\infty}} \quad (6)$$

According to this model, when the cavity collapse, the velocity at the wall would become infinity. Rayleigh [23] recalculated bubble collapse and limited the collapse velocity. Plesset [24] expanded this equation and include vapour pressure, which is also referred to as Linear Rayleigh Equation or simplified RP equation.

$$R = \sqrt{\left(\frac{2|P_v - P_\infty|}{3\rho}\right)} \quad (7)$$

Later Plesset [24] included the surface tension and vapour pressure effect, which is generally referred to as Rayleigh-Plesset (RP) bubble dynamic equation.

$$R \frac{d^2R}{dt^2} + \frac{3}{2} \left(\frac{dR}{dt}\right)^2 + \frac{4\mu}{R} \frac{dR}{dt} + \frac{2\sigma}{\rho R} = \frac{P_b - P_\infty}{\rho} \quad (8)$$

where R is the bubble radius, $\frac{dR}{dt}$ is the bubble wall velocity, σ is the surface tension and P_v is the vapour pressure.

The bubble dynamic equation proposed by the other researcher has been listed in Table 2. Although a simplified form of the Rayleigh-Plesset (RP) equation is widely adopted in cavitation modelling, particularly with the mixture, Volume of Fluid (VOF) and Eulerian-Eulerian multi-phase approach.

Table 2. Different Forms of Bubble dynamic equation

Author	Equation	Remarks
Knapp et al. [25]	$P = P_v - \frac{2\sigma}{R} + \frac{NT}{R^3}$	Include the effect of Ideal gas in the cavity. It is useful to predict cavitation inception.
Kato et al. [26]	$\frac{\partial T}{\partial t} + \frac{dR}{dt} \left(\frac{R}{r}\right)^2 \frac{\partial T}{\partial t}$ $= \alpha \left(\frac{\partial^2 T}{\partial r^2} + \frac{2}{r} \frac{\partial T}{\partial r}\right)$	This model includes thermal & inertial effects in bubble collapse.

3.2.2. Cavitation Modelling

The classification of multi-dimensional cavitation modelling is not easy, broadly it can be categorised into two groups (i) Continuum models and (ii) Interface tracking models. Interface capture is a more promising technique, in which the liquid and vapour phase is treated separately. There are individual equations for continuity and momentum that have been solved for each phase, which required more computational time. Rider and Kothe [27] estimated that interface tracking methods required six times the computational cost of the continuum model. In the continuum model, the two phases are considered to be the same fluid. Often, liquid viscosity, surface tension and relative velocity are neglected, and the pressure of the mixture is assumed to be the saturation pressure. The continuum method is a more convenient way of modelling cavitation.

(a) Single Fluid Model

The Volume of Fluid (VOF) & Mixture multiphase model consists similar governing equation by considering both phases simultaneously. The vapour fraction conservation equation estimates the phase change process in the mixture model. The VOF method comprises a secondary equation of volume fraction, apart from Navier-Stokes equations and turbulence model equation.

The summation of the volume fraction of two phases is equal to unity and thus satisfied the continuity equation. This model was originally proposed by Hirt and Nichols [28] and a transport equation based on liquid volume fraction can be given as:

$$\frac{\partial(\alpha_l \rho_l)}{\partial t} + \nabla \cdot (\alpha_l \rho_l U) = 0 \quad (9)$$

where U , α_l and ρ_l are the mixture velocity, volume fraction and density of liquid, respectively. The VOF required a very fine mesh to capture the interface, therefore the applications of this model for cavitation flow in fuel nozzle are still limited.

(b) Barotropic Model

If the change in the fluid density is considered to be the only function of pressure difference, i.e. $\rho = \rho(p)$, known as Barotropic flow. It implies that the bubble will immediately alter in volume in a two-phase cavitation flow with a modest pressure difference. Different versions of Barotropic models have been proposed by Kubota et al. [29], Delannoy and Kueny et al. [30], Chen and Heister [31], Avva et al. [32], and Schmidt et al. [33].

One of the initial cavitation models proposed by Kubota et al. [29] considers cavitation as a cluster of small bubbles, of identical size and uniformly distributed. He has specified the bubble number density & the initial bubble radius. This model is reasonable for large scale with low Mach number cavitation flow. Delannoy and Kueny [30] assumed that the density was a function of pressure (Barotropic flow) and all the phases are in thermodynamic equilibrium (HEM-Homogeneous Equilibrium Model) at all times. They solved continuity and Euler's equation (i.e. Navier-Stokes equation without viscous diffusion term) and simulated water flow through the venturi. In the intermediate phase (Liquid vapour mixture), the density was changed with pressure following a sine curve. They also conclude that in the absence of interphase, it could be considered an incompressible flow. They achieved reasonably good qualitative results, but deviate from quantitative results from the experiments.

Later Chen and Heister [31] excluded the idea of one-to-one mapping of density and pressure and argued that the pressure field should be related to the density history. Because of the consideration of a time effect, density and pressure are not connected by an equation of state. They came up with a relation for the pressure of a cloud of tiny bubbles on the assumption that there were a set number of bubbles per unit mass. However, their methodology is not appropriate for small-scale applications like fuel injector flow. Avva et al. [32] proposed an enthalpy-based model and used an energy equation.

The results obtained with this model are reasonably matched with experimental data, but they reported problems with the model's stability hence limited to very low upstream pressure conditions. Schmidt et al. [33] proposed a compressible pseudo-density model for cavitation flow. Their model considers the compressibility of both pure phases, which allows the wave motion in the fluid. They used mass, momentum balance equation and algebraic equation of state for closer hydrodynamic equations.

The equation of state was derived from the enthalpy transport equation. This model is preferable for high-pressure fuel injector flow. Schmidt's barotropic Homogeneous Equilibrium Model (HEM) has been adopted by other researchers. It has been implemented in OpenFOAM® [35], which is utilized by Salvador et al. [34]. However, Schmidt et al. [33] and Salvador et al. [34] both have neglected the turbulence effect. They considered that with a very small length scale, cavitation overwhelms the turbulent effect. Reitz et al. [36] include turbulence with HEM and implemented it in KIVA-3V [37].

(c) Mass Transport Model

The mass transport model also referred to as the Baroclinic model, used the equation of state in combination with a transport equation for liquid and gas volume fractions. A mass transport equation including a cavitation source term. This model is more accurate to find the physical details of the cavitation phenomena and modelling the detachment of cavity bubbles. There is various mass transport model which has been proposed by a researcher with different source term i.e. Merkle et al. [38], Kunz et al. [39], Schnerr and Sauer [40], Singhal et al. [41], and Zwart et al. [42]. To estimate the phase change between liquid and vapour with this model a source term is required in the mass transport equation.

$$\frac{\partial(\alpha_l \rho_l)}{\partial t} + \nabla \cdot (\alpha_l \rho_l U) = R_c + R_e \quad (10)$$

where R_c and R_e are the rates of mass transfer source terms for condensation and evaporation, respectively. U , α_l and ρ_l are the mixture velocity, volume fraction and density of liquid, respectively. If there is no mass transfer between phases, RHS is zero, which is the transport equation for the Volume of Fluid (VOF) model.

Merkle et al. [38] and Kunz et al. [39] proposed a pressure-based model for the condensation and evaporation rate to take into account the mass transfer between the two phases. In their source term equation, only the liquid phase contributes to vaporization, therefore, only α_l has been seen.

In both model presence of non-condensable gases and turbulence was measured, however, surface tension and the viscous effect was not considered. These models' main drawback is the large variety of tuning parameters that depend on the different sorts of applications. Schnerr-Sauer [40] proposed a simplified VOF or dispersed VOF and implement Linear Rayleigh Equation to calculate the mass transfer rate. Surface tension and non-condensable gases were not taken into account in this model.

Singhal et al. [41] developed a full cavitation model based on Equal Velocity and Equal Temperature (EVET) based on bubble dynamics. They were considered non-condensable gas, which was dissolved and present in the liquid. They included the surface tension(σ) and turbulent kinetic energy (k) in the source term equations.

To calculate the overall interphase mass transfer rate per unit volume, Zwart et al. [42] assumed a uniform bubble size. Their model was based on the linear Rayleigh equation, and they also ignore the presence of non-condensable gas.

Table 3. Different mass transfer source terms for condensation and evaporation

Authors	Source term for Evaporation ($P_l < P_v$) and Condensation rate ($P_v < P_l$)
Merkle et al. [38]	$R_e = C_{dest} \frac{\alpha_l \rho_l \min [0, P_l - P_v]}{t_{\infty} \rho_v (0.5 \rho_l U_{\infty}^2)}, (C_{dest}=1)$ $R_c = C_{prod} \frac{(1-\alpha_l) \max [0, P_l - P_v]}{t_{\infty} \rho_v (0.5 \rho_l U_{\infty}^2)}, (C_{prod}=80)$
Kunz et al. [39]	$R_e = C_v \frac{\alpha_l \rho_v \min [0, P_l - P_v]}{t_{\infty} \rho_v (0.5 \rho_l U_{\infty}^2)}, (C_v=100)$ $R_c = C_c \frac{(1-\alpha_l) \alpha^2 \rho_v}{t_{\infty}}, (C_c=100)$
Schnerr and Sauer [40]	$R_e = -C_v \frac{3 \rho_l \rho_v \alpha_l (1-\alpha_l)}{\rho_m R_b} sgn(P_l - P_v) \sqrt{\frac{2 P_l - P_v }{3 \rho_l}}$ $R_c = C_c \frac{3 \rho_l \rho_v \alpha_l (1-\alpha_l)}{\rho_m R_b} sgn(P_v - P_l) \sqrt{\frac{2 P_l - P_v }{3 \rho_l}}$
Singhal et al. [41]	$R_e = C_e \frac{\sqrt{k}}{\sigma} \rho_l \rho_v \left[\frac{2(P_v - P_l)}{\rho_l} \right]^{0.5} - (1 - f_v - f_g), (C_e=0.02)$ $R_c = C_c \frac{\sqrt{k}}{\sigma} \rho_l \rho_v \left[\frac{2(P_v - P_l)}{\rho_l} \right]^{0.5} f_v, (C_c=0.01)$
Zwart et al. [42]	$R_e = F_{vap} \frac{3 \alpha_{nuc} \rho_v (1-\alpha_v)}{R_b} \sqrt{\frac{2 P_l - P_v }{3 \rho_l}}, (F_{vap}=50)$ $R_c = F_{con} \frac{3 n_0 \rho_v}{R_b} \sqrt{\frac{2 P_l - P_v }{3 \rho_l}}, (F_{con}=0.01)$

(d) Two-fluid model

In the two-fluid model, liquid and gas treat separately and the governing equations are solved for both phases. This model can be divided into two groups of approaches: i.e. Eulerian-Eulerian approach & the Eulerian-Lagrangian approach. The Eulerian-Eulerian approach considers liquid and gas phases in the Eulerian frame of reference. Yuan and Schnerr [43] implemented this approach with CICSAM (compressive interface capturing scheme for arbitrary meshes) method for interface capturing. They consider all three phases' i.e. non-condensable gas, vapour and liquid. Alajbegovic et al. [44] solved a set of mass, momentum, and turbulence equations for each phase of cavitation by treating it as a single mixture with the Linear Rayleigh Equation. They initially predicted a constant bubble number density, but later they updated the model to take the vapour volume fraction into account. Battistoni et al. [45] implemented his model in AVL Fire® [46] which is similar to that of Alajbegovic et al. [44]. They used two different methods for the treatment of bubble number density. (i) Mono-dispersed: All bubbles consider the same in size, (ii) Poly-dispersed: Bubbles are of variable size. They observe that the Mono-dispersed approach is preferable, as it requires less computational time without compromising accuracy. The poly-dispersed approach is more suitable to study cavitation erosion due to bubble collapse.

The liquid is viewed as a continuum or carrier phase in the Eulerian frame of reference and the vapour bubbles are viewed as discrete or dispersed phases in the Lagrangian frame of reference in the Eulerian-Lagrangian approach. When one of the two phases has a low volumetric concentration or is naturally distributed, this method is preferred. Giannadakis et al. [47] developed the Eulerian-Lagrangian model to simulate cavitation in a fuel injector nozzle. The model takes into account interactions between bubbles, bubble expansion and contraction, turbulent bubble dispersion, and hydrodynamic disintegration. The model was validated with the experimental results of Arcoumaniset al. [13] of real size nozzle. Sou et al. [48] also used the Eulerian-Lagrangian approach and coupled it with the Rayleigh-Plesset equation. They simulated with a Large Eddy Simulation (LES) turbulent model and validate results with the in-house experiment of large size nozzle with a rectangular cross-section.

Due to significant improvements in computational processors, the use of commercial CFD tools increases in recent times, which allows an understanding of the hydrodynamic behaviour of the cavitation flow in detail. There are different commercial tools are available particularly FLUENT, CONVERGE, AVL-Fire, and Open Foam reported by various researchers. It is also equally important to validate the results obtained from a new model or method implemented in CFD software with experimental data. Experimental work published by Winklhofer et al. [14] is mostly used for validation due to very comprehensive information in terms of quantitative as well as qualitative results.

Mohan et al. [49], Saha et al. [50], He et al. [51], Rojas et al. [52], Zhao et al. [53], and Payri et al. [54] validated their model or methods with Winklhofer's experimental data obtained for two-dimensional throttle geometry. A detailed summary of the work carried out in different CFD software by the various researchers is listed in Table 4.

Table 4. Summary of the work carried out in different CFD tool by the various researchers

Author	Operating pressure, Nozzle dimension	CFD tool	Work detail
Payri et al. [55]	$P_{inj}=1000$ bar, $P_{back}=80$ bar	ANSYS-Fluent	Compared cylindrical & conical nozzle geometry for cavitation
Som et al. [56]	$D=0.169$ mm $P_{inj}=800-1600$ bar, $P_{back}=1$ bar	ANSYS-Fluent	Injection pressure, needle lift position and fuel type were analyzed for inner nozzle cavitation flow
Vijayakumar et al. [57]	$D=0.169$ mm, $\gamma=120^0$ $P_{inj}=1100$ & 1300 bar, $P_{back}=30$ bar	ANSYS-Fluent (SS, k- ϵ)	Calculated C_d for Diesel and blend of Diethyl ether fuels to study the cavitation flow.
Battistoni et al. [58]	$D=0.5$ mm & $L=2.5$ mm $P_{inj}=10.6$ bar, $P_{back}=0.87$ bar	CONVERGE & AVL-Fire	Compared the homogenous mixture model+VOF(implement in CONVERGE) with the multi-fluid non-homogenous model (implement on AVL-Fire) to investigate the cavitation flow.
Battistoni et al. [59]	$D_i=0.145$ mm, $D_o=0.13$ mm, $L=1$ mm $P_{inj}=780$ bar, $P_{back}=20$ bar	CONVERGE (VOF, HRM, RANS)	Compared mass flow rate with available experimental measurement & the effects of needle off-axis motion during the injection event has been studied
Salvador et al. [60,61]	$D_{mid}=0.125$, $D_o=0.156, 0.17, 0.18$ mm $L=0.57$ mm $P_{inj}=400$ bar, $P_{back}= 10$ to 250 bar	OpenFOAM (HEM, RANS)	Discharge coefficient (C_d), area coefficient (C_a) and velocity coefficient (C_v) is estimated with different convergence-divergence levels to understand the cavitation flow.
Yu et al. [62]	$D_i-D_m-D_o=0.155-0.165-0.162$ mm $P_{inj}=1100, 700, 300$ bar, $P_{back}=40$ bar	OpenFOAM (VOF, SS, LES)	Calculate mass flow rates, momentum fluxes, effective injection velocity, and discharge coefficient while taking compressibility into account for various injection situations.
Ahmed et al. [63]	Square hole of 1.94 mm $P_{inj}=22-28$ bar	OpenFOAM (VOF, SS, LES)	Considered non-condensable and uses the interphase capturing method.

4. Influence of Cavitation Flow on Spray Characteristics

Reitz [64,65] elaborated the fuel atomization process in two steps: near nozzle primary break-up and downstream secondary breakup, shown in Fig 10. Liquid fuel comes out in the form of continuous flow up to a finite distance from the nozzle exit, beyond which the primary break-up starts due to flow instability, further breakup of droplets into smaller droplets referred to as a secondary breakup. The internal flow strongly influences the spray characteristics reported by various researchers. Although the effect of cavitation on the droplet size distribution, spray angle etc is still not satisfactorily analysed.

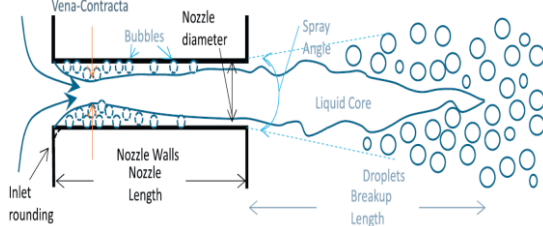


Figure 10. Sketch of the atomization processes of liquid fuel injected from a nozzle, Reitz [64]

Huh and Gosman [66] proposed a phenomenological or one-dimensional model. The cavitation inside the nozzle hole is attributed to turbulent fluctuation at the exit flow being the source of perturbation to the free surface. They correlate the spray angle with turbulence quantities at the nozzle outlet. They also extend their work and correlate spray break-up with turbulence but do not include the cavitation effect.

Arai et al. [67,68,69] found that the spray characteristics change dramatically and the atomization can be enhanced with the presence of cavitation bubbles from the inlet to the exit of a nozzle. The collapse of the cavitation bubble promotes the liquid jet breakup. The geometry of the nozzle and the pressure boundary conditions affect the cavitation's structure. If the length of the nozzle is long enough, the cavitation bubble does not reach the nozzle exit. In this case, He and Ruiz [70] found that cavitation still influences the downstream flow field by adding turbulent intensity within the flow. Arcoumanis et al. [71] proposed a spray model considering the effect of upstream conditions i.e. transient fuel injection behaviour, turbulence and nozzle cavitation. The model includes several constants to estimate the nozzle discharge and primary breakup. This model offers an important step in the coupling of nozzle flow to the downstream spray prediction.

In a similar theme, Sarre et al. [72] produced a model for a multidimensional spray with the help of cavitating and non-cavitating nozzle flow regimes maps.

4.1. Cavitation Coupled Spray Model

Comprehensive multidimensional cavitation coupled spray model has evolved recently, due to the requirement of high computational cost. There are two different approaches researchers are following. The first one is the two-step approach, where two separate calculations using the Eulerian model to simulate cavitation inside nozzle flow and the Lagrangian approach for the outside injector for the spray region. In this method, discrete particles are superimposed on the continuous gas phase. Reitz [73] proposed a linear phenomenological or one-dimensional model in which, liquid droplets consider 'blobs' are injected at the outlet of the nozzle and are applied to account for the primary breakup. The model's consistency at near nozzle flow is poor due to an inherently weak connection to the inner nozzle flow. Berge et al. [74,75], Som et al. [76,77,78], and Wang et al. [79] predicted the near nozzle flow by considering the effect of nozzle turbulence & cavitation on the primary breakup. Berge et al. [74] developed a methodology to couple spray and internal nozzle flow at AVL and applied it within the framework of FIRE CFD code. They adopt a two-fluid model for cavitation flow and a Discrete Droplet Model (DDM) for spray simulation. Som et al. [78] implemented KH-ACT (Kelvin Helmholtz-Aerodynamic Cavitation Turbulence) model in CONVERGE® [80] to simulate spray characteristics of diesel and bio-diesel and compared it with data from Sandia National Laboratory. Battistoni et al. [81] reported similar work by using the result of the first computing step, mapped at the nozzle exit area, for the initialization of the primary breakup model.

In the second approach, both liquid and vapour are considered in the continuum phase and the conservation laws are solved under Eulerian flow assumptions. This required grid refinement up to the sub-micron level to detect droplets without injecting any discrete particles. Lebas et al. [82] used DNS (Direct Numerical Simulation) and Oley et al. [83] conducted the simulation with LES (Large Eddy Simulation). This approach is also termed as 'quasi-DNS', however, its application is limited due to its high computation cost. Salvador [84] proposed Σ -Y Eulerian coupled model implemented in CONVERGE® software. This model has been validated with the results of Spray A and Spray-C from the Engine Combustion Network (ECN). Spray A is a non-cavitating nozzle with a high k-factor and a convergent diameter of 90 μm . In contrast, Spray C is a cavitating nozzle with a constant diameter of 200 μm and a k-factor of 0. The validated models are used to examine the flow conditions and spray characteristics at the nozzle outlet for the elliptical nozzles. This includes factors such as mass flow, momentum flux, liquid and vapour fractions, radial and axial velocity

profiles, as well as spray features such as spray angle, air entrainment, and spray tip penetration. Despite the various methods reported recently, a rigorous and realistic method to simulate both the internal cavitation flow and spray formation is yet to be reported. In this case, experimental work can be useful to understand the effect of cavitation flow on the spray characteristics.

4.2. Experimental Study on Cavitation-Induced Spray Breakup

Sou et al. [85,86], Suh and Lee [87], Bicer et al. [88], and Abderrezzak [89] conducted a thorough study to examine the impact of cavitation on spray characteristics using a 2D transparent acrylic nozzle geometry. They employed nozzles of different length-to-width ratios. The nozzle geometry has a significant effect on spray characteristics i.e. spray cone angle and ligament formation. They also observed that super-cavitation, where vapour bubbles are swept outside the nozzle exit, had a considerable effect on the atomization characteristics. Most of the experimental study has been carried out with the transparent 2D nozzle so that they could allow visualization of cavitation inside the nozzle. There is still a considerable lack of information on the influence of cavitation with the use of real-size 3D nozzles on spray formation. Payri et al. [90,91,92] and Desantes et al. [93] conducted the experimental and numerical studies to measure the effect of cavitation on the velocity, mass flux and momentum flux at the exit of the bi-orifice nozzle. For this study, they have used two different nozzles (i) Cylindrical and (ii) Conical. They concluded that the cavitation produces a substantial increase in a spray cone angle. The shear stress between the nozzle wall & fluid will decrease due to the presence of cavitation. However, there is limited visualization information regarding the development of cavitation flow. The captured images are not very clear to distinguish the different regimes of cavitation and their effect on liquid atomization. Abbasiaslet al. [94] used a micro-scale nozzle to visualize cavitation, and the effect of cavitation on spray is investigated in terms of cone angle, droplet size distribution and droplet velocity distribution. They observed that the spray angle improved during developing cavitation and super-cavitation regimes but drop significantly during the cavitation flip, as shown in Fig. 11.

Hwang [95] provided an in-depth analysis of the interaction of cavitation with sprays in high-pressure diesel injection systems. The author discussed various experimental techniques used to study cavitation in diesel fuel injection systems, such as high-speed imaging, X-ray radiography, and acoustic measurements. The author also described various mathematical models used to simulate cavitation in

fuel injection systems, including empirical models, numerical models, and analytical models.

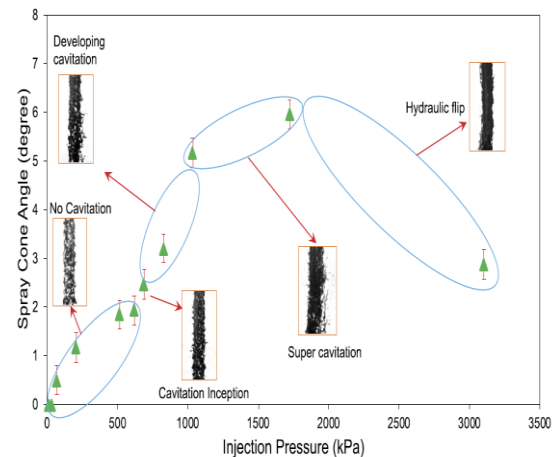


Figure 11. Spray cone angle with different cavitation flow pattern map, Abbasiaslet al. [94]

5. Vortex induced cavitation

Recent research has identified two different types of cavitation, which have been further defined as geometry-induced cavitation and vortex-induced cavitation or string-type cavitation as shown in Fig. 12. It is believed that cavitation bubbles can be found within the low-pressure region of a highly-organized, large-scale vortex structure that develops in regions with high vorticity. The phenomenon of geometric-induced cavitation occurs at sharp corners where the pressure is lower than the vapor pressure of the liquid. On the other hand, string or vortex cavitation occurs in the bulk of the liquid of sac or min sac-type nozzles, where large-scale vortices can be formed due to the available volume relative to the nozzle geometry. Gavaises et al. [96] characterized the string cavitation by using 15 times enlarge 6 holes transparent cylindrical and tapered nozzle ($d_{in}=2.8$ mm, $d_{out}=2.5$ mm, $L=15$ mm). It is found that the String cavitation emerges in regions where large-scale vortices form, originating from either pre-existing geometric cavitation sites or trapped air downstream of the hole exit. Small variations in the shape of the needle and needle eccentricity have been found to significantly affect the cavitation strings. The study by Cao et al. [97] aimed to investigate the effect of fuel temperature and different cavitation patterns on the development of cavitation inside diesel injector nozzles. The experiments were conducted using a transparent two-hole injector nozzle ($d_{in}=2.1$ mm, $d_{out}=2$ mm, $L=10$ mm) and shadow photography. They observed the String-type cavitation at 1 mm of needle lift and Sheet-type cavitation caused by the geometry of the near-wall region occurs as the needle lift to 2 mm. The results showed that the string-type cavitation was more sensitive to fuel temperature and had a significant impact on the spray angle and

penetration, while the sheet-type cavitation had a minor effect on the spray characteristics and was less sensitive to the fuel temperature.

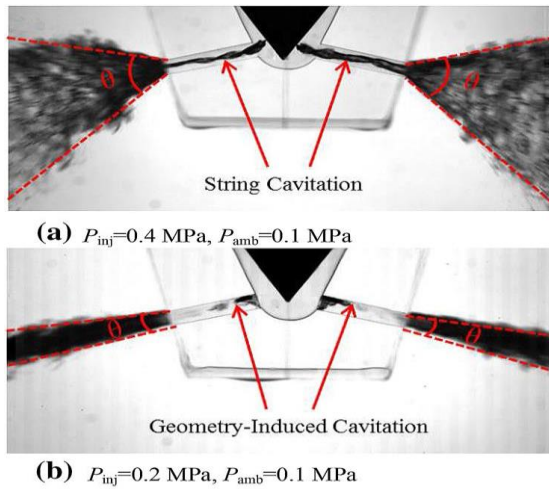


Figure 12. Two types of cavitation patterns obtained by shadow photography, Cao et al. [97]

Prasetya et al. [98] and Nurcholik et al. [99] explored the three-dimensional structure of the string cavitation by using an enlarged three-hole cylindrical mini-sac cylindrical nozzle ($d=2$ mm, $L=8$ mm). They used tomographic-stereo particle image velocimetry (TSPIV) to obtain flow structure under different needle lift conditions ($Z/D=0.5, 1$ & 3). When needle lift is high ($Z/D=3$) the vertical velocity gradient is low, which makes it harder to form string cavitation. At $Z/D=1$, twin string cavitation swirling flow was observed. At a low needle lift ratio of $Z/D=0.5$, a single stable string cavitation with a larger diameter is produced by a steady swirling flow upstream of an orifice. This swirling flow creates a steady spiral flow in the orifice and a hollow-cone spray, resulting in a notable increase in spray angle. Guan et al. [100] performed experimental and numerical studies to characterise string-type cavitation in real-size tapered nozzles ($d_{in}=0.33$ mm, $d_{out}=0.26$ mm, $L=1.84$ mm). The diesel fuel was used to inject at an injection pressure of 60 MPa. They performed numerical simulations by using a three-phase VOF model with the SS cavitation model in the ANSYS-Fluent platform. The results show that the vortex flow can significantly alter the cavitation shape and length, while the cavity intensity is relatively insensitive to the vortex flow. According to the analysis based on the equation for vorticity transport, the main factor in the creation and growth of string cavitation is the stretching of the vortex. The impact of the dilatation term, which is connected to the compressibility of the fluid, is of lesser importance, followed by the effect of the baroclinic torque term on the distribution of vorticity. Wei et al. [101] also used real size tapered shape nozzle to understand cavitation flow and near-field spray under multiple injections. The author

investigated the impact of multiple injections on the internal flow and spray characteristics in the vicinity of the nozzle, specifically focusing on how needle valve throttling and pressure fluctuations at the nozzle inlet contributed to these effects. They found that the spray cone angle and the spray area ratio increase slowly in the form of "boot-shaped", followed by a sudden increase during the main injection. The string cavitation is observed when the position of the needle valve shifts and the spray cone angle increases suddenly. Kumar et al. [102] performed a numerical study by using 20 times scaled-up mini-sac type six-hole injector nozzle ($d=3.5$ mm). They implemented a mixture multiphase model with a ZGB cavitation model in ANSYS-Fluent. They successfully captured the vortices structure by using the RANS turbulence model. According to the analysis, two primary types of vortex structures were observed. The first type of structure, referred to as "hole-to-hole" connecting vortices, is formed by connecting two neighbouring holes. The second type of structure, characterized by double counter-rotating vortices, originated from the needle wall and entered the injector hole opposite to it.

Gavaises et al. [103] presented a numerical investigation of fuel dribbling and wall-wetting phenomena in a multi-hole diesel injector nozzle. The simulations were carried out using a commercial CFD software ANSYS Fluent, with a two-phase Eulerian-Lagrangian approach. The movement of air is modelled using an extra equation for transport, which is linked with the VOF interface capturing technique to accurately represent the atomization process near the nozzle, and to capture the effects of the liquid spray on the nozzle walls. The model incorporates a pre-defined movement of the needle inside the VCO nozzle along both the axial and eccentric directions, utilizing an immersed boundary technique called the IBM. It is observed that the vortex or string cavities are created from the needle surface to the orifice exit, while small droplets and ligaments are formed near the nozzle exit region. The swirling flows inside the orifices are intensified due to the needle's eccentric motion, which plays a key role in breaking up the injected liquid jet into ligaments and directing them backwards towards the external wall of the injector. The study reveals that wall-wetting effects are more noticeable when the valve is closing and fuel injection is occurring in subsequent events. This is due to the presence of residual gases trapped in the nozzle, which facilitate the complete atomization of the injected fluid.

Recently, Yang et al. [104] reviewed the effect of cavitating flow in the liquid nitrogen spray cooling state. The cavitation in cryogenic fluids involves mass transfer as well as heat transfer due to the evaporation of the liquid phase. It is observed that the droplet size and its distributions are the major factors during heat and mass transfer. The heat transfer occurs between droplets and the heated surface. The

efficiency of spray cooling depends on the evaporation characteristics of the droplets. When dealing with cryogenic droplets, the temperature difference between the heat source and the droplets is relatively large, leading to quick evaporation and intricate interaction between the two phases.

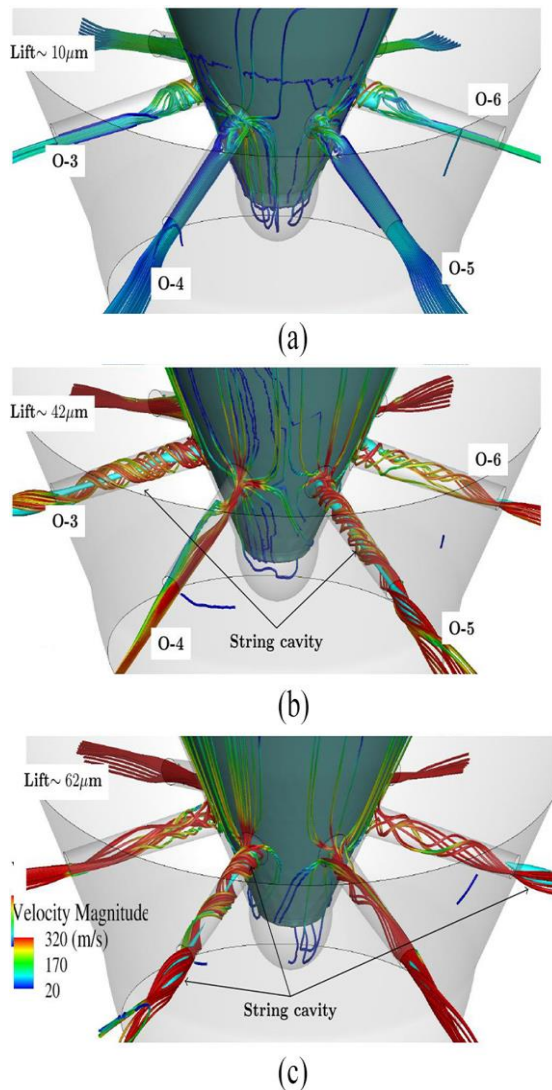


Figure 13. String cavitation at selected needle lift during the SOI, Gavaises et al. [103]

Conclusions

Modern injectors for passenger cars and heavy-duty engines inject liquid fuel through the orifice of diameter in the order of 100 to 300 μm , with 2000 bar injection pressure. During high-pressure injection, fuels flowing inside the fuel injector nozzle holes observed the cavitation phenomenon. The cavitation flow has a predominant effect on the near nozzle flow. It is very important to understand the characteristics of the cavitation flow and its effect on spray formation. This paper summarizes the recent experimental and computational work and derived the following conclusion.

- The conclusion drawn from the literature is that cavitation flow exhibits distinct flow regimes. Cavitation inception occurs at the nozzle entrance, followed by the growth and extension of cavitation bubbles to the nozzle exit with an increase in fuel injection pressure, resulting in supercavitation. However, a further increase in injection pressure can lead to the creation of a thin layer of gas at the nozzle wall, causing the cavitation to disappear immediately, which is referred to as a hydraulic flip.
- The observation of cavities in small-scale nozzles and bubble clouds in large-scale nozzles indicates that the length scales of bubbles are independent of the nozzle's length scale. Interestingly, the size of the nozzle was found to not affect the coefficient of discharge.
- Experimental results suggest that the classical scaling theory does not always accurately predict the behavior of cavitation flow. The scale effect appears to be influenced by a range of factors, including liquid quantity, bubble dynamics, geometrical differences caused by wall roughness, specific flow regimes, and cavitation nuclei. In realistic operating conditions, super-cavitation has been observed instead of hydraulic flip in full-scale nozzles.
- The visualization of nozzle flow has been carried out using various techniques such as Schlieren methods, shadowgraph technique, interferometry imaging, Laser Doppler velocimetry (LDV), X-ray computed tomography (CT), X-ray radiography, laser light sheet illumination, and high-speed CCD cameras. However, the use of a transparent nozzle has limitations on the maximum injection pressure due to the high material stress generated within the nozzle wall. To facilitate higher injection pressures, a transparent 2D nozzle embedded in a steel sheet has been utilized to visualize the internal flow.
- The one-dimensional cavitation model proposed by Nurik [9] is preferably good to predict the discharge coefficient with a sharp inlet nozzle but does not give much detail about the internal flow behaviour of the cavitation phenomena. The experimental data are consistent with this one-dimensional model. The effect of rounding at the inlet increases C_d and the data falls above the theoretical curve.
- The classification of multi-dimensional cavitation modeling is challenging, but it can broadly be divided into two groups: (i)

Continuum models and (ii) Interface tracking models. Continuum models treat the liquid-vapor mixture as a single phase, while interface tracking models treat the liquid and vapor phases separately. Interface tracking models are more accurate but require six times the computational cost of the continuum model. The dynamic behavior of the bubble can be determined by the Rayleigh-Plesset (RP) equation, which describes the bubble's response to external pressure fluctuations.

- The cavitation flow is a complex phenomenon that involves bubble formation, coalescence, and breakup, which are influenced by the local pressure distribution and the interaction of the flow field with bubbles. Accurate modelling of all these features is challenging and most existing models make inherent assumptions by ignoring the effect of non-condensable gases, turbulence, compressibility, and surface tension. To overcome these limitations, more advanced modelling techniques that account for these factors are required.
- It is observed that the spray characteristics change dramatically and the atomization process is improved in the presence of cavitation from the inlet to the exit of a nozzle. The collapse of the cavitation bubble promotes the liquid jet breakup. It is concluded that the spray angle improved during developing cavitation and super-cavitation regimes but dropped significantly during the cavitation flip.
- Comprehensive multidimensional cavitation coupled spray model has evolved recently, however, the requirement of computational cost is very high. In this case, experimental work can be more useful to understand the effect of cavitation flow on the spray characteristics.
- The string cavitation is observed when the position of the needle valve shifts or at a lower needle lift and the spray cone angle increases significantly. It is also observed that string cavitation is more sensitive to the fuel temperature as compared to geometry-induced cavitation.

Nomenclature

A_1	Inlet cross-sectional area [m ²]
A_2	Outlet cross-sectional area [m ²]
C_c	Coefficient of contraction
C_d	Discharge coefficient
d	Nozzle diameter [mm]
\dot{m}	Mass flow rate [kg/s]

K	Cavitation parameter
k	Turbulent kinetic energy [J/kg]
P	Pressure [Pa]
P_{back}	Downstream pressure of the nozzle [Pa]
P_{inj}	Injection pressure of the nozzle [Pa]
P_v	Vapour pressure [Pa]
R_c	Rate of mass transfer source term for condensation [kg/s]
R_e	Rate of mass transfer source term for evaporation [kg/s]
R	Bubble radius [mm]
R_0	Initial bubble radius [mm]
t	Bubble collapse time [s]
U	Mixture velocity [m/s]
u	Flow velocity [m/s]

Greek letters

α	Volume fraction [-]
ρ	Density [kg/m ³]
σ	Surface tension [N/m ²]
μ	Dynamic viscosity [N/ms]

Subscript

back	Back
c	Condensation
crit	Critical
e	Evaporation
in	Inlet
inj	Injection
l	Liquid
mid	Middle
o	Outlet
v	Vapour

Abbreviations

CCD	Charge-coupled device
CICSAM	Compressive interface capturing scheme for arbitrary meshes
CFD	Computational fluid dynamics
CN	Cavitation number
CT	Computed tomography
DNS	Direct Numerical Simulation
EVET	Equal Velocity Equal Temperature
LDA	Laser Doppler Anemometry
LDV	Laser Doppler Velocimetry
LES	Large Eddy Simulation
HEM	Homogeneous Equilibrium Model
KH-ACT	Kelvin Helmholtz-Aerodynamic Cavitation Turbulence
PIV	Particle image velocimetry
RANS	Reynolds average Navier Stroke
RP	Rayleigh-Plesset
SDM	Satur mean diameter
SCA	Spray cone angle
SLE	Selective Laser Etching
STP	Spray tip penetration
SS	Schnerr-Sauer
VOF	Volume of fluid

Conflict of Interest

We declare that there is no conflict of interest regarding the publication of this manuscript. In addition, We have entirely observed the ethical issues, including plagiarism, informed consent, misconduct, data fabrication and/or falsification, double publication and/or submission, and redundancy.

References

- [1] ExxonMobil., 2014. The Outlook for Energy: A view to 2040. Technical report.
- [2] Scitesch, G., 2003. Modeling engine spray and combustion process. New York: Springer.
- [3] Baumgarten, C., 2006. Mixture formation in internal combustion engines. Springer Science & Business Media.
- [4] Brennen, C. E., 2014. Cavitation and bubble dynamics. Cambridge University Press.
- [5] Schmidt, D. P., &Corradini, M. L., 2001. The internal flow of diesel fuel injector nozzles: a review. International Journal of Engine Research, 2(1), 1-22.
- [6] Franc, J. P., & Michel, J. M., 2006. Fundamentals of cavitation. Springer Science & Business Media.
- [7] Cui, J., Lai, H., Feng, K., & Ma, Y., 2018. Quantitative analysis of the minor deviations in nozzle internal geometry effect on the cavitating flow. Experimental Thermal and Fluid Science, 94, 89-98.
- [8] Bergwerk, W., 1959. Flow pattern in diesel nozzle spray holes. Proceedings of the Institution of Mechanical Engineers, 173(1), 655-660.
- [9] Nurick, W. H., 1976. Orifice cavitation and its effect on spray mixing. ASME Journal of Fluids Engineering, 98(4), 681-687.
- [10] Soteriou, C., Andrews, R., & Smith, M., 1995. Direct injection diesel sprays and the effect of cavitation and hydraulic flip on atomization. SAE transactions, (950083).
- [11] Chaves, H., Knapp, M., Kubitzek, A., Obermeier, F., & Schneider, T., 1995. Experimental study of cavitation in the nozzle hole of diesel injectors using transparent nozzles. SAE transactions, (950504).
- [12] Schmidt, D. P., Rutland, C. J., Corradini, M. L., Roosen, P., &Genge, O., 1999. Cavitation in asymmetric two-dimensional nozzles. Journal of Engines, 108(3), 613-629.
- [13] Arcoumanis, C., Flora, H., Gavaises, M., &Badami, M., 2000. Cavitation in real-size multi-hole diesel injector nozzles. SAE transactions, (2000-01-1246).
- [14] Winklhofer, E., Kull, E., Kelz, E., &Morozov, A., 2001. Comprehensive hydraulic and flow field documentation in model throttle experiments under cavitation conditions. In Proceedings of the ILASS-Europe conference, Zurich 2001 (pp. 574-579).
- [15] Payri, R., Salvador, F. J., Gimeno, J., & Venegas, O., 2013. Study of cavitation phenomenon using different fuels in a transparent nozzle by hydraulic characterization and visualization. Experimental Thermal and Fluid Science, 44, 235-244.
- [16] Sou, A., Maulana, M. I., Hosokawa, S., &Tomiyama, A., 2008. Ligament formation induced by cavitation in a cylindrical nozzle. Journal of Fluid Science and Technology, 3(5), 633-644.
- [17] Mauger, C., Méès, L., Michard, M., Azouzi, A., &Valette, S., 2012. Shadowgraph, Schlieren and interferometry in a 2D cavitating channel flow. Experiments in fluids, 53(6), 1895-1913.
- [18] Cui, J., Lai, H., Feng, K., & Ma, Y., 2018. Quantitative analysis of the minor deviations in nozzle internal geometry effect on the cavitating flow. Experimental Thermal and Fluid Science, 94, 89-98.
- [19] Kirsch, V., Hermans, M., Schönberger, J., Ruoff, I., Willmann, M., Reisgen, U., ...&Reddemann, M. A., 2019. Transparent high-pressure nozzles for visualization of nozzle internal and external flow phenomena. Review of Scientific Instruments, 90(3), 033702.
- [20] Weisbach, J., 1882. Mechanics of engineering: Theoretical mechanics, with an introduction to the calculus. D. Van Nostrand.
- [21] Lichtarowicz, A., Duggins, R. K., & Markland, E., 1965. Discharge coefficients for incompressible non-cavitating flow through long orifices. Journal of mechanical engineering science, 7(2), 210-219.
- [22] Reitz, R. D., 1978. Atomization and other breakup regimes of a liquid jet. Princeton University.
- [23] Rayleigh, L., 1917. On the pressure developed in a liquid during the collapse of a spherical cavity. The London, Edinburgh, and Dublin Philosophical Magazine and Journal of Science, 34(200), 94-98.
- [24] Plesset, M. S., 1949. The dynamics of cavitation bubbles. Trans. ASME, J. Appl. Mechanics, 16, 228-231.
- [25] Knapp, R. T., Daily, J. W., &Hammit, F. G., 1970. Cavitation. McGraw-Hill.
- [26] Kato, H., Kayano, H., &Kageyama, Y., 1994. A consideration of thermal effect on cavitation bubble growth. American Society of

- Mechanical Engineers, New York, NY (United States).
- [27] Rider, W., & Kothe, D., 1995. Stretching and tearing interface tracking methods. In 12th computational fluid dynamics conference.
- [28] Hirt, C. W., & Nichols, B. D., 1981. Volume of fluid (VOF) method for the dynamics of free boundaries. *Journal of computational physics*, 39(1), 201-225.
- [29] Kubota, A., Kato, H., & Yamaguchi, H., 1989. Finite difference analysis of unsteady cavitation on a two-dimensional hydrofoil. In *International Conference on Numerical Ship Hydrodynamics*, 5th.
- [30] Delannoy, Y., & Kueny, J. L., 1990. Two phase flow approach in unsteady cavitation modelling. *ASME Journal Fluids Engineering Division (FED)*, 98, 153-158.
- [31] Chen, Y., & Heister, S. D., 1995. Two-phase modeling of cavitated flows. *Computers & Fluids*, 24(7), 799-809.
- [32] Avva, R. K., Singhal, A. K., & Gibson, D. H., 1995. An enthalpy based model of cavitation. *ASME-PUBLICATIONS-FED*, 226, 63-70.
- [33] Schmidt, D. P., Rutland, C. J., & Corradini, M. L., 1999. A fully compressible, two-dimensional model of small, high-speed, cavitating nozzles. *Atomization and sprays*, 9(3).
- [34] Salvador, F. J., Hoyas, S., Novella, R., & Martínez-López, J., 2011. Numerical simulation and extended validation of two-phase compressible flow in diesel injector nozzles. *Proceedings of the Institution of Mechanical Engineers, Part D: Journal of Automobile Engineering*, 225(4), 545-563.
- [35] Open CFD Ltd., 2014. OpenFOAM, Documentation.
- [36] Ning, W., Reitz, R. D., Diwakar, R., & Lippert, A. M., 2008. A numerical investigation of nozzle geometry and injection condition effects on diesel fuel injector flow physics. *SAE Technical Paper*.
- [37] Los Alamos National Laboratory. 1999. KIVA-3V Manual.
- [38] Merkle, C. L., 1998. Computational modelling of the dynamics of sheet cavitation. In *Proc. of the 3rd Int. Symp. on Cavitation*, Grenoble, France.
- [39] Kunz, R. F., Boger, D. A., Stinebring, D. R., Chyczewski, T. S., Lindau, J. W., Gibeling, H. J., Venkateswaran, S., & Govindan, T. R., 2000. A preconditioned Navier-Stokes method for two-phase flows with application to cavitation prediction. *Computers & Fluids*, 29(8), 849-875.
- [40] Schnerr, G. H., & Sauer, J., 2001. Physical and numerical modeling of unsteady cavitation dynamics. In *Fourth International Conference on Multiphase Flow, ICMF New Orleans*.
- [41] Singhal, A. K., Athavale, M. M., Li, H., & Jiang, Y., 2002. Mathematical basis and validation of the full cavitation model. *Journal of Fluids Engineering*, 124(3), 617-624.
- [42] Zwart, P. J., Gerber, A. G., & Belamri, T., 2004. A two-phase flow model for predicting cavitation dynamics. In *Fifth International Conference on Multiphase Flow*, Yokohama, Japan.
- [43] Yuan, W., & Schnerr, G. N., 2003. Numerical simulation of two-phase flow in injection nozzles: Interaction of cavitation and external jet formation. *Journal of Fluids Engineering*, 125(6), 963-969.
- [44] Alajbegovic, A., Greif, D., Basara, B., & Iben, U., 2003. Cavitation calculation with the two-fluid model. In *3rd European-Japanese Two-Phase Flow Group Meeting*, Certosa di Pontignano.
- [45] Battistoni, M., & Grimaldi, C. N., 2010. Analysis of transient cavitating flows in diesel injectors using diesel and biodiesel fuels. *SAE International Journal of Fuels and Lubricants*, 3(2), 879-900.
- [46] AVL. Fire@ Documentation.
- [47] Giannadakis, E., Gavaises, M., & Arcoumanis, C., 2008. Modelling of cavitation in diesel injector nozzles. *Journal of Fluid Mechanics*, 616, 153-193.
- [48] Sou, A., Biçer, B., & Tomiyama, A., 2014. Numerical simulation of incipient cavitation flow in a nozzle of fuel injector. *Computers & Fluids*, 103, 42-48.
- [49] Mohan, B., Yang, W., & Chou, S., 2014. Cavitation in injector nozzle holes—a parametric study. *Engineering Applications of Computational Fluid Mechanics*, 8(1), 70-81.
- [50] Saha, K., & Li, X., 2016. Assessment of cavitation models for flows in diesel injectors with single-and two-fluid approaches. *Journal of Engineering for Gas Turbines and Power*, 138(1).
- [51] He, Z., Zhang, L., Saha, K., Som, S., Duan, L., & Wang, Q., 2017. Investigations of effect of phase change mass transfer rate on cavitation process with homogeneous relaxation model. *International Communications in Heat and Mass Transfer*, 89, 98-107.
- [52] Sanmiguel-Rojas, E., Gutierrez-Castillo, P., delPino, C., & Auñón-Hidalgo, J. A., 2019. Cavitation in transient flows through a micro-nozzle. *Journal of Fluids Engineering*, 141(9).

- [53] Sanmiguel-Rojas, E., Gutierrez-Castillo, P., delPino, C., & Auñón-Hidalgo, J. A., 2019. Cavitation in transient flows through a micro-nozzle. *Journal of Fluids Engineering*, 141(9).
- [54] Payri, R., Gimeno, J., Martí-Aldaraví, P., & Martínez, M., 2021. Validation of a three-phase Eulerian CFD model to account for cavitation and spray atomization phenomena. *Journal of the Brazilian Society of Mechanical Sciences and Engineering*, 43(4), 1-5.
- [55] Payri, R., Margot, X., & Salvador, F. J., 2002. A numerical study of the influence of diesel nozzle geometry on the inner cavitating flow. SAE paper.
- [56] Som, S., Longman, D. E., Ramírez, A. I., & Aggarwal, S. K., 2010. A comparison of injector flow and spray characteristics of biodiesel with petrodiesel. *Fuel*, 89(12), 4014-4024.
- [57] Thulasi, V., & Rajagopal, T. K., 2013. Study of Internal Flow Characteristics of Injector Fuelled with Various Blends of Diethyl Ether and Diesel Using CFD Study of Internal Flow Characteristics of Injector Fuelled with Various Blends of Diethyl Ether and Diesel Using CFD. *Frontiers in Heat and Mass Transfer (FHMT)*, 4(2).
- [58] Battistoni M, Som S, Longman DE., 2014. Comparison of mixture and multifluid models for in-nozzle cavitation prediction. *Journal of Engineering for Gas Turbines and Power*, 136(6).
- [59] Battistoni M, Xue Q, Som S, Pomraning E., 2014. Effect of off-axis needle motion on internal nozzle and near exit flow in a multi-hole diesel injector. *SAE international Journal of Fuels and Lubricants*, 7(1):167-82.
- [60] Salvador FJ, Martínez-López J, Caballer M, De Alfonso C., 2013. Study of the influence of the needle lift on the internal flow and cavitation phenomenon in diesel injector nozzles by CFD using RANS methods. *Energy conversion and management*, 66:246-56.
- [61] Salvador FJ, Jaramillo D, Romero JV, Roselló MD., 2017. Using a homogeneous equilibrium model for the study of the inner nozzle flow and cavitation pattern in convergent-divergent nozzles of diesel injectors. *Journal of Computational and Applied Mathematics*. 2017 Jan 1;309:630-41.
- [62] Yu H, Goldsworthy L, Brandner PA, Li J, Garaniya V., 2018. Modelling thermal effects in cavitating high-pressure diesel sprays using an improved compressible multiphase approach. *Fuel*. 2018 Jun 15;222:125-45.
- [63] Ahmed A, Duret B, Reveillon J, Demoulin FX., 2020. Numerical simulation of cavitation for liquid injection in non-condensable gas. *International Journal of Multiphase Flow*. 2020 Jun 1;127:103269.
- [64] Reitz RD. Atomization and other breakup regimes of a liquid jet. Princeton University; 1978.
- [65] Reitz RD. Mechanism of breakup of round liquid jets. *Encyclopedia of fluid mechanics*. 1986.
- [66] Huh K, Gosman AD. Atomization mechanism of fuel injection. ICLASS-90, Hartford, Connecticut. 1990.
- [67] Arai M. Similarity between the break-up lengths of a high-speed liquid jet in atmospheric and pressurized conditions. *Proc. of ICLASS-91*. 1991.
- [68] Hiroyasu H., 1991. Break-up length of a liquid jet and internal flow in a nozzle. In *Proc. 5th. ICLASS 1991*, pp. 275-282.
- [69] Arai M. Break-up mechanisms of a high-speed liquid jet and control methods for a spray behavior. *ISASC-94*. 1994.
- [70] He L, Ruiz F. Effect of cavitation on flow and turbulence in plain orifices for high-speed atomization. *Atomization and sprays*. 1995;5(6).
- [71] Arcoumanis C, Gavaises M, French B., 1997. Effect of fuel injection processes on the structure of diesel sprays. *SAE transactions*. 1997 Jan 1:1025-64.
- [72] von Kuensberg Sarre C, Kong SC, Reitz RD., 1999. Modeling the effects of injector nozzle geometry on diesel sprays. *SAE transactions*. 1999 Jan 1:1375-88.
- [73] Reitz RD., 1987. Modeling atomization processes in high-pressure vaporizing sprays. *Atomisation Spray Technology*. 1987;3(4):309-37.
- [74] Berg EV, Edelbauer W, Tatschl R, Volmajer M, Kegl B, Alajbegovic A, Ganippa L., 2003. Validation of a CFD model for coupled simulation of nozzle flow, primary fuel jet break-up and spray formation. In *Internal Combustion Engine Division Spring Technical Conference 2003 Jan 1*, Vol. 36789, (pp. 171-180).
- [75] Berg EV, Edelbauer W, Alajbegovic A, Tatschl R., 2003. Coupled calculation of cavitating nozzle flow, primary diesel fuel break-up and spray formation with an Eulerian multi-fluid-model. In *Proc. 9th International Conference on Liquid Atomisation and Spray Systems (ICLASS'03) 2003 Jul* (pp. 12-02).
- [76] Som S, Ramirez AI, Aggarwal SK, Kastengren AL, El-Hannouny E, Longman DE, Powell CF, Senecal PK., 2009. Development and validation of a primary breakup model for diesel engine

- applications. SAE Technical Paper; 2009 Apr 20.
- [77] Som S., Aggarwal S., 2009. Assessment of atomization models for diesel engine simulations. *Atomization and Sprays*. 2009;19(9).
- [78] Som S., Aggarwal SK., 2010. Effects of primary breakup modeling on spray and combustion characteristics of compression ignition engines. *Combustion and flame*. 2010 Jun 1;157(6):1179-93.
- [79] Wang Y, Ge HW, Reitz RD., 2010. Validation of mesh-and timestep-independent spray models for multi-dimensional engine CFD simulation. *SAE International Journal of Fuels and Lubricants*. 2010 Jan 1;3(1):277-302.
- [80] Richards KJ., Senecal PK., 2008. Pomraning E. CONVERGE™ (Version 1.2) manual. Middleton, WI: Convergent Science, Inc.
- [81] Battistoni M., Grimaldi C., Mariani F., 2012. Coupled simulation of nozzle flow and spray formation using diesel and biodiesel for CI engine applications. SAE Technical Paper; 2012 Apr 16.
- [82] Lebas R., Menard T., Beau PA., Berlemont A., 2009. Demoulin FX. Numerical simulation of primary break-up and atomization: DNS and modelling study. *International Journal of Multiphase Flow*. 2009 Mar 1;35(3):247-60.
- [83] Örley F, Trummer T, Hickel S, Mihatsch MS, Schmidt SJ, Adams NA. Large-eddy simulation of cavitating nozzle flow and primary jet break-up. *Physics of Fluids*. 2015 Aug 21;27(8):086101.
- [84] Salvador, F. J., Pastor, J. M., Gomez-Soriano, J., & Martínez-Miracle, E. C., 2023. Performance of elliptical nozzles on the spray dynamics of convergent and constant section nozzles by means of a Σ -Y coupled model. *Fuel*, 346, 128259.
- [85] Sou, A., Hosokawa, S., & Tomiyama, A., 2007. Effects of cavitation in a nozzle on liquid jet atomization. *International Journal of Heat and Mass Transfer*, 50(17-18), 3575-3582.
- [86] Sou, A., Minami, S., Prasetya, R., Pratama, R. H., Moon, S., Wada, Y., & Yokohata, H., 2015. X-ray visualization of cavitation in nozzles with various sizes. In ICLASS-15.
- [87] Suh, H. K., & Lee, C. S., 2008. Effect of cavitation in nozzle orifice on the diesel fuel atomization characteristics. *International Journal of Heat and Fluid Flow*, 29(4), 1001-1009.
- [88] Biçer, B., & Sou, A., 2016. Application of the improved cavitation model to turbulent cavitating flow in fuel injector nozzle. *Applied Mathematical Modelling*, 40(7-8), 4712-4726.
- [89] Abderrezzak, B., & Huang, Y., 2016. A contribution to the understanding of cavitation effects on droplet formation through a quantitative observation on breakup of liquid jet. *International Journal of Hydrogen Energy*, 41(35), 15821-15828.
- [90] Payri, F., Bermúdez, V., Payri, R., & Salvador, F. J., 2004. The influence of cavitation on the internal flow and the spray characteristics in diesel injection nozzles. *Fuel*, 83(4-5), 419-431.
- [91] Payri, R., García, J. M., Salvador, F. J., & Gimeno, J., 2005. Using spray momentum flux measurements to understand the influence of diesel nozzle geometry on spray characteristics. *Fuel*, 84(5), 551-561.
- [92] Payri, R., Salvador, F. J., Gimeno, J., & Venegas, O., 2013. Study of cavitation phenomenon using different fuels in a transparent nozzle by hydraulic characterization and visualization. *Experimental Thermal and Fluid Science*, 44, 235-244.
- [93] Desantes, J. M., Payri, R., Salvador, F. J., & Soare, V., 2005, April 11. Study of the influence of geometrical and injection parameters on diesel sprays characteristics in isothermal conditions. SAE Technical Paper.
- [94] Abbasiasl, T., Niazi, S., Aghdam, A. S., Chen, H., Cebeci, F. Ç., Ghorbani, M., Grishenkov, D., & Koşar, A., 2020. Effect of intensified cavitation using poly (vinyl alcohol) microbubbles on spray atomization characteristics in microscale. *AIP Advances*, 10(2), 025318.
- [95] Hwang, J., 2021. Interaction of Cavitation with Sprays in High-Pressure Diesel Injection Systems. In *Cavitation and Bubble Dynamics* (pp. 249-264). Academic Press.
- [96] Gavaises, M., Andriotis, A., Papoulias, D., Mitroglou, N., & Theodorakakos, A., 2009. Characterization of string cavitation in large-scale Diesel nozzles with tapered holes. *Physics of Fluids*, 21(5), 052107.
- [97] Cao, T., He, Z., Si, Z., EL-Seesy, A. I., Guan, W., Zhou, H., & Wang, Q., 2020. Optical experimental study on cavitation development with different patterns in diesel injector nozzles at different fuel temperatures. *Experiments in Fluids*, 61, 1-14.
- [98] Prasetya, R., Sou, A., Oki, J., Nakashima, A., Nishida, K., Wada, Y., ...& Yokohata, H., 2021. Three-dimensional flow structure and string cavitation in a fuel injector and their effects on discharged liquid jet. *International Journal of Engine Research*, 22(1), 243-256.

- [99] Nurcholik, S. D., Sou, A., Miwa, T., Kawaguchi, M., Matsumoto, Y., Nishida, K., & Ueki, Y., 2023. Single and twin string cavitation swirling flows in multi-hole mini-sac diesel injector and sprays. *Journal of Fluid Science and Technology*, 18(2), JFST0023-JFST0023.
- [100] Guan, W., He, Z., Zhang, L., Guo, G., Cao, T., & Leng, X., 2021. Investigations on interactions between vortex flow and the induced string cavitation characteristics in real-size diesel tapered-hole nozzles. *Fuel*, 287, 119535.
- [101] Wei, Y., Fan, L., Zhang, H., Gu, Y., Deng, Y., Leng, X., ...& He, Z., 2022. Experimental investigations into the effects of string cavitation on diesel nozzle internal flow and near field spray dynamics under different injection control strategies. *Fuel*, 309, 122021.
- [102] Kumar, A., Ghobadian, A., & Nouri, J., 2022. Numerical simulation and experimental validation of cavitating flow in a multi-hole diesel fuel injector. *International Journal of Engine Research*, 23(6), 958-973.
- [103] Gavaises, M., Murali-Girija, M., Rodriguez, C., Koukouvini, P., Gold, M., & Pearson, R., 2022. Numerical simulation of fuel dribbling and nozzle wall wetting. *International Journal of Engine Research*, 23(1), 132-149.
- [104] Yang, X., Xue, R., Wang, N., Huang, Z., Zhang, H., Liu, X., ...& Hou, Y., 2023. Review of internal cavitating flow in injection nozzles, external atomization and cooling in liquid nitrogen spray cooling systems. *Cryogenics*, 103661.
- [105] Manin, J., Yasutomi, K., & Pickett, L. M., 2018. Transient cavitation in transparent diesel injectors (No. SAND2018-3668C). Sandia National Lab.(SNL-NM), Albuquerque, NM (United States).
- [106] Knox-Kelecy, A. L. (Doctoral dissertation, The University of Wisconsin-Madison). Turbulent flow in a scale model of a diesel fuel injector nozzle hole.
- [107] Ohn, T. R., Senser, D. W., & Lefebvre, A. H., 1991. Geometric effects on spray cone angle for plain-orifice atomizers. *Atomization and Sprays*, 1(3).
- [108] Gelalles, A. G., 1930. Coefficients of discharge of fuel injection nozzles for compression-ignition engines. US Government Printing Office.